

Will Iron Forge the Future of Metal-Air Batteries in Grid Scale Energy Storage?

Katerina Bogomolov^[a, b] and Yair Ein-Eli^{*[a, b, c]}

The community is exploring sustainable alternatives for grid-scale energy storage. Besides lithium-ion batteries (LIBs), such technologies with a focus on sustainability aspects offer only a limited solution for grid-scale energy storage. Rechargeable metal-air batteries (MABs) based on affordable abundant multivalent metal anodes in aqueous medium provide promising theoretical metrics, such as volumetric capacity, but do not completely fulfill their potential when scaled from lab to commercial products. Both the metal anode and the air cathode need to be addressed: corrosion, hydrogen evolution reaction (HER) during charging, and passivation all diminish the anode's effective volumetric energy density and shelf life, while the air

cathode's challenges include sluggish kinetics, low efficiency, and poor stability. Nevertheless, this Perspective highlights iron-air MABs as an appealing sustainable alternative for grid-scale energy storage, since iron is abundant and affordable, recyclable, has multielectron reversible redox activity, historically rich experience in production and processing, and is safe to handle. Given that further research will be directed to exploring the composition and design of electrolytes and electrodes, it may lead to advances in scaling and commercialization, as well as reducing the environmental impact of secondary batteries utilized for grid-scale energy storage in the next decades.

1. An Overview

The desire to find innovative side-by-side battery technologies^[1] to lithium-ion batteries (LIB) and the rising trend of addressing sustainability set the path to developing new technologies based on abundant multivalent chemistries. In tandem, tremendous efforts are invested in grid-scale energy storage devices to capture the most out of the generated energy, increasing non-fluctuating continuity and availability on demand by renewable power sources, i.e. wind, hydro-based and solar. However, the road to making them the primary source of energy is still bumpy. Cost-effectiveness of lab-developed alternatives remains to be a significant issue as the implementation of the proposed solutions, when it comes to practical scaled scenarios, includes more considerations, e.g. geopolitical, cost fluidity of raw materials and logistics, production facility, process engineering, regulations and market demand. Nonetheless, to realize this transition, batteries should provide key parameters, i.e. energy and power density, prolonged cycle life and sustainability.

2. Limitations of Li-Ion Batteries for Stationary Energy Storage

Li-ion batteries (LIBs) continue to be a global leader in the deployment of rechargeable batteries for the grid scale energy storage market.^[2,3] The preceding three decades featured major advances in this industry, including increasing energy density alongside decreasing expenditures. However, there are significant restrictions to consider when embracing them as a stationary energy storage alternative. Although this technology has a higher energy efficiency (85–95%) than the current leading greener solution, pumped storage hydropower (65%–80%),^[3] its cost is still twice as much, exceeding the target set by the US Department of Energy (100 \$/kWh)^[4,5] and those stated in EU-funded projects, like Batteries Europe and Battery 2030+ (≤ 100 €/kWh).^[6–8] Furthermore, it should be noted that lithium practical availability is limited by the supply chain and more particularly by the resource scarcity,^[9] thus, the rapidly growing market of electric vehicles and portable devices with the same battery chemistry further reduces the accessibility of resources.^[10] The latter is especially crucial for stationary applications which require some gravimetric energy density but obligates minimal volumetric energy density, since raw material reduction can be an essential factor in spatial restrictions, power management, and cost.^[3,11] Another consideration is the cycle life, since any battery energy storage technology falls short of hydropower, which is predicted to last at least half a century.^[3] Overall, it can be challenging to compare this aspect of the two systems since leveled cost of energy storage is dependent on fluid parameters such as installation, operation hours, maintenance, and input power pricing.^[12] Nonetheless, the cycle life restriction encompasses deterioration of the composing elements, resulting in discarding of defective modules. Unfortunately, the widespread utilization of lithium

[a] Department of Materials Science and Engineering, Technion – Israel Institute of Technology, Haifa Israel

[b] Israel National Institute for Energy Storage (INIES), Technion – Israel Institute of Technology, Haifa Israel

[c] The Nancy & Stephan Grand Technion Energy Program (GTEP) Technion – Israel Institute of Technology Haifa Israel

Correspondence: Yair Ein-Eli, Department of Materials Science and Engineering, Technion – Israel Institute of Technology, Haifa 3200003 Israel. Email: eineli@technion.ac.il

© 2025 The Author(s). ChemSusChem published by Wiley-VCH GmbH. This is an open access article under the terms of the Creative Commons Attribution Non-Commercial License, which permits use, distribution and reproduction in any medium, provided the original work is properly cited and is not used for commercial purposes.

for both established electromobility and rising stationary applications imposes not only techno-economic challenges but also sustainability related concerns.^[13,14] Meeting energy generation and energy transition demands poses safety and chain-value related concerns. The safety concern relates to the possibility of thermal runaway, which might have disastrous repercussions if a stationary energy storage facility caught fire. This may introduce not only liabilities issues but also severe environmental impact in the form of a pollution.^[15]

Figure 1 presents greenhouse gas emissions (GHG) for selected grid-scale technologies. The chain value issue is somewhat more complicated. First, while the environmental footprint of GHG during manufacturing is proportional to the mass of the battery produced, high energy density batteries require fewer resources to produce the same value of energy, implying a reduced carbon footprint on a facility scale. A cradle-to-gate GHG emissions per storage capacity presented by Jiao et al.^[17] reveals that quantitatively, LIBs exceed pumped storage hydropower emissions by 36–80%. While the main contributors vary, the recycling process is the largest contributor to the former's emissions. Owing to the relatively short operation life in comparison to the pumped hydropower listed previously, periodic replacement is required. The last argument emphasizes the absence of standards regarding end-of-life^[18] and the disparity in the recycling rate, not only in the early phases of LIBs in the stationary field, as they serve currently less than a decade, but also in the well-established non-stationary market. This fact necessitates securing future supply by replacing virgin materials with a growing share of recycled materials, as rising demand calls for the use of excess raw resources, constraining geopolitically the supply chain, while recycling has effectively low rate and efficiency. Pyrometallurgy, hydrometallurgy, and direct recycling are examples of currently industrially established recycling procedures to support circular economy by recovering valuable metals, i.e. Li, Co and Ni.^[19] Nonetheless, these processes are rather costly due to waste purification, emission, process complexity and safety regulation.^[20] These aspects establish a gap between the specified targets for using materials derived from wasted LIBs and the actual recycled content.^[19]

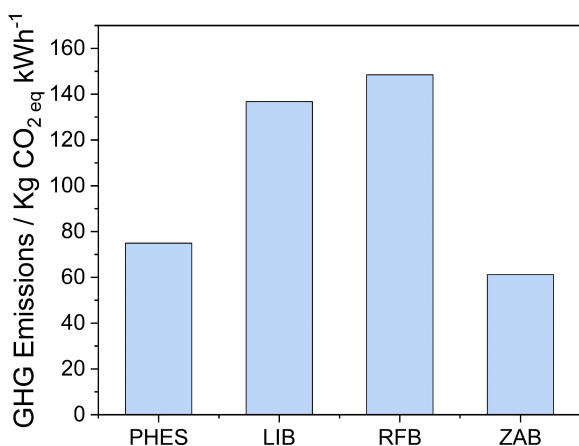


Figure 1. GHG emissions for selected grid-scale technologies, based on.^[16,17]

3. Grid-Scale Battery Alternatives: RFBs and MABs

This pivots the focus to develop alternative solutions for Li-ion batteries in the framework of battery technology for grid-scale energy storage. RFBs and MABs are the two emerging contemporary alternatives. Both concepts are distinctive from the conservative cell architecture.^[21–23]

In RFBs, energy is stored within the electrolyte medium, i.e. the active materials are dissolved and stabilized salts, stored in external reservoir tanks rather than in a solid-state electrode.^[24,25] The cell itself is still based on two compartments, fed by the external tanks with the catholyte and the anolyte and separated by an ion-selective membrane to ensure adequate functioning during the redox process.^[22] This structure entails the ability to some extent to separate between the energy and power performance. Whereas mass transport and surface area have great impact on the latter, tank volume and salt concentration have the most impact on the former.^[25] On the one hand, this attribute delivers the necessary degree of flexibility for modularity and scalability, which has led to the commercial maturation of this technology.^[5] However, these properties are still interdependent via viscosity.^[26] Higher concentrations increase viscosity, which reduces conductivity while also increasing the energy losses due to drag and polarization.^[22,26] Nonetheless, this technology encounters additional practical challenges when scaled for grid-scale energy storage applications. First, one must consider that external reservoirs dictate the energy density to be relatively low.^[5,22] Second, considering the dynamic nature of renewable power sources, flow rate can be adjusted to match fluctuating demands, however it effectively implies that efficiency will be modified.^[22] Faster flow rates reduce ion starvation and enhance the value of the limiting current, yet it may also result in higher pump losses and an imbalance between feed rate and active material consumption.^[27,28] Third, cost-effectiveness is dictated by the price of the salts as derived from their purity, the additives,^[22,29,30] used to control the viscosity, solubility, mass transfer, the catalysts, used to reduce the resistivity and hydrophobicity, minimize the activation, reduce parasitic reactions, such as hydrogen and oxygen evolution, or to enhance the effective surface area, and the ion-selective membrane.^[31–33] its selectivity, permeability, ionic conductivity, and stability. where the last has been assigned to the highest cost share relative to overall cell, and its production is questionable in terms of sustainability.^[34] Fourth, dual chemistries frequently degrade through crossover and poisoning.^[35,36] Singular chemistries that address this issue retain three to four valencies while these ionic species remain stable within the electrolyte's electrochemical stability range. The constraints are in fact strict and limit the alternatives to a handful selection. All-vanadium RFBs are well known, although they likewise suffer from sensitivity to low purity active materials^[37] and undesirable reactions that result in precipitation and blocking.^[38]

The second alternative, MABs, is also atypical. The uniqueness is attributed to the architecture of the porous cathode,

where just as in the previous alternative, this half-cell operates on an external reservoir, however in this case the active material in this compartment is oxygen, supplied from the air or a purified feedstock.^[39–41] Furthermore, despite being much less commercially mature for grid-scale compared to the previous type, these batteries have received increasing attention in the electrochemical research community primarily due to their high theoretical volumetric capacity with allegedly dirt-cheap price when anodes are based on abundant metals available in the earth crust.^[42] The common choices for the anode include elements such as alkali metals (Li, Na, K), alkaline earth metals (Mg) and metalloids (Si, Al) or transition metals (Zn, Fe).^[40,43] This variety has a prospective theoretical energy density that puts Li-ions batteries at disadvantage (410 Wh Kg^{-1} for conventional LCO/C Li-ion cell^[44,45] compared to different MAB combinations, see Figure 2a and b).

Inevitably, the reactivity of alkali metals drives researchers to nonaqueous aprotic electrolytes and room temperature ionic liquids with high interest for minimizing moisture sensitivity via oxygen feed dehydration.^[46,47] It immediately spikes the cost and shifts the focus back to the safety issue.^[48,49] Furthermore, typical carbonate-based electrolytes for Li-ion batteries are out of the question since they easily react with the produced oxygen intermediates during discharge.^[50,51] Generally, these intermediates tend to react parasitically not only with the electrolyte but also with the cathode support and binder, resulting in the accumulation of passivating precipitated by-products such as alkyl carbonates.^[52,53] Specifically for Li-air, the mechanism of discharge involves formation of unstable superoxide that disproportionate chemically into peroxide. It is necessary to direct the route toward solution-phase growth rather than surface dominated in order to support reversible recharging that is not hampered by passivation.^[50]

The other two alkali alternatives present better reversibility, since the formed superoxide is stable. Tragically, the cathodes suffer from superoxide buildup during cycling, limiting oxygen

transport which cuts the capacity shortly after only decent cycling.^[50] The anodes suffer from detrimental gradual irreversible dendrite growth, resulting in not only active material loss but also a risk of battery cyclability termination due to shorts and damaged solid-electrolyte interphase, resulting in excessive electrolyte consumption.^[58,59] The solutions offered are adapting the intercalation-type anodes, but they leads to a reduction in the specific energy, and in scenarios of alkali metal with relatively high ionic radius, it deteriorates the anode through exfoliation.^[46,60]

Unlike alkali metal-based MABs, possessing noteworthy reversibility and considered environmentally friendly, only a few of the previously designated elements can be considered as rechargeable (electrically or mechanically) and operate stably in aqueous medium; Zn is the most prevalent, then Fe (discussed in Section 4), with Mg and Al staggering behind.^[41,61] Aqueous electrolytes are nonflammable, have favorable conductivity, and given their affordability, they are extremely adaptable since their properties can be readily adjusted by altering the pH or introducing additives, inducing from small kinetic adjustments to complete mechanism variation.^[62,63] In these electrolytes, although Mg and Al offer potentially higher battery voltage, specific energy, and volumetric energy density, compared to Zn, lower reactivity considered Li,^[40] and higher abundance considered both,^[43] they share a common intrinsic disadvantage as anodes: relative fast corrosion and parasitic reactions.^[64,65] The first is exhibited as major self-discharge that gradually stimulates passivation and imposes significant polarization loss, shifting the practical battery voltage to approximately the same range as any typical rechargeable aqueous battery. The second challenge, namely HER, is reflected in performance as low coulombic efficiency. This parasitic reaction, an occurrence associated with the operation of many anodes in aqueous media, not only reduces cell's efficiency, but is also structurally damaging MABs, since excessive accumulated hydrogen increases the internal pressure.^[66] Pressure buildup has a negative

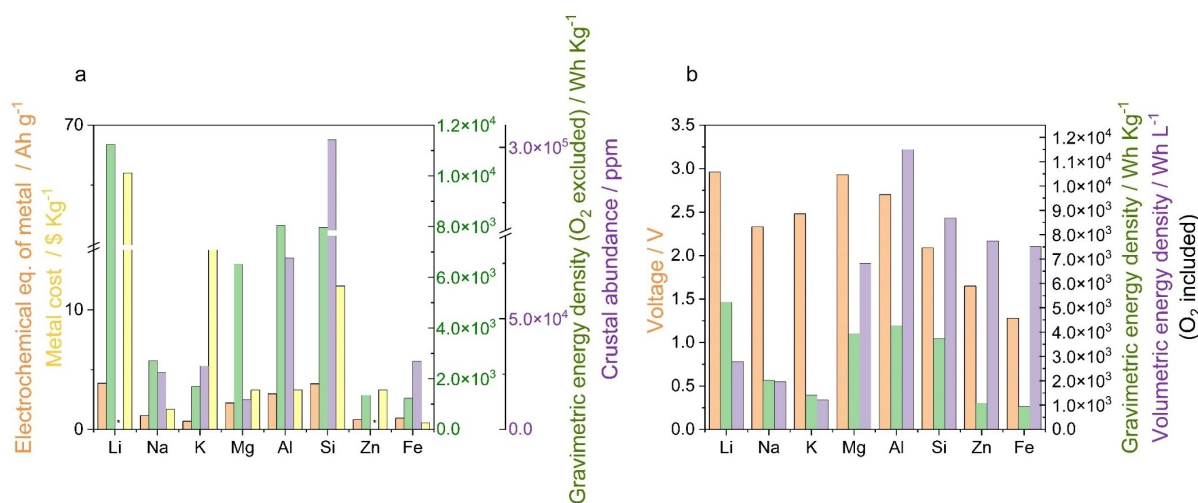


Figure 2. (a) Electrochemical eq. of metal specific capacity (sp, in Ah g^{-1}),^[45] gravimetric energy density (calculated: $\text{gED} = V \cdot \text{sp}$, O_2 excluded), Crustal abundance (* lithium and zinc abundance is 22 and 52 respectively)^[54] and metal cost (highest were considered),^[55–57] (b) voltage,^[43,45,56] gravimetric energy density (calculated: $\text{gED} = V \cdot \text{sp}$) and volumetric energy density (calculated: $\text{vED} = V \cdot \text{sp} \cdot \rho$), (O_2 included).^[58]

impact on battery performance, as it triggers electrolyte leakage^[67] and flooding of the gas diffusion layer of the air-cathode,^[66,68] resulting in unstable and damaged triple-phase boundaries (electrolyte-gaseous oxygen-catalyst interface).

Silicon is on the one hand the most tempting for realization, but is uniquely challenging. While the EU considers Si to be a critical raw material, the US seems to discount it. The cause is economic strategic reliance on supply rather than actual resource depletion,^[69] as the mineral commodity summaries 2024 state that Si and its alloys are abundant in the majority of producing nations worldwide,^[70] which is sensible given that it is the second most abundant element in the earth's crust.^[54] Currently, this chemistry is considered primary rather than secondary, while mechanical recharging permits its reuse.^[71] In aqueous electrolytes, reversibility is restricted by the solubility of discharge products, i.e. silicates; when the local concentration is surpassed, passive silicon dioxide forms on the anode, causing polarization losses. The activity of Si, which is critical for efficient discharge, is also intrinsically challenging since once the anode is exposed to the electrolyte, a simultaneous corrosion process occurs, forming an additional silicon-based layer that only partially prevents water molecules from reaching the surface.^[71] Hence, the corrosion process continues, and hydrogen gas evolved from the active surface, disrupts the partially formed passive layer. This process exposes additional active surface, leading to a continuous vicious cycle of passivation renewal and breakage. These co-processes are responsible for inherent voltage instability. Non-aqueous electrolytes, especially ionic liquids, provide some relief from the corrosion and carbonation issues posed by aqueous electrolytes while also providing a wider electrochemical stability window as compared to aqueous media. The disadvantage is that the electrolytes are more expensive, as well as having lower ionic conductivity and viscosity, which are critical for the air-cathode. Additionally, in these media low discharge current unexpectedly results in low capacity, and vice versa; this phenomenon is specific to the size of the produced discharge deposits.^[72] At low current density, the deposits are finer and clog the porous air electrode more extensively, preventing further oxygen transfer and limiting the effective active surface area. Practically, despite being innovative and drawing an extensive amount of academic attention, this type of chemistry is not yet technologically ready for commercialization as a rechargeable MAB since it is primary, its energetic efficiency is half due to low operative voltage, and the discharge rate is slow.^[43,71]

On the contrary, Zn is already commercially mature for primary and secondary MABs for small-scale applications, however: it falls short of grid-scale requirements and faces fundamental interconnected challenges including corrosion, passivation, dendritic growth, and parasitic HER.^[73,74] Unlike Mg, Al, and Si, these challenges are at present considered more manageable. Yet, whereas lab-scale research provides a glimpse at process level electrochemically, scaling calls for a focus on performance, criteria that are frequently overlooked, such as stacking, individual cell design, realistic testing regimes, reproducibility, and cost-driven evaluation, including material choice, electrode dimensions, active to inactive material ratio

and electrolyte volume.^[74] Nonetheless, to the best of our knowledge, commercially grid scale Zn-air batteries are in their early stages, with multiple pioneering companies, including E-Zinc, AZA battery, Zinc8 and Phinergy, offering microgrid products that have already been scaled to some extent.^[75]

Currently, the market has no solution that can fulfill the requirements for batteries for grid scale energy storage, as demonstrated in Figure 3. The green vacant space in the Figure illustrates that there is currently no battery capable of providing the cost-effective performance necessary for **grid-scale** applications.^[3] As previously stated, pumped hydropower storage energy storage system is the most dominant solution. It surely complies to this vacant space; however, comparing it to the accessible and the developing battery-based solutions, i.e. LIBs, RFBs, and MABs, is challenging since it holds energy reservoirs ranging from megawatts to gigawatts, allowing for low margin cost per kWh.^[3,78] Yet, accompanying expenses rise from installation, energy management and maintenance. Additionally, this system is thought to be geographically bound since it requires specific land contours and water source,^[78,79] unlike batteries. Nonetheless, MABs are the nearest to surpass the thresholds for cost and energy density.

This paragraph highlights that chemistries based on abundant multivalent elements accommodated in aqueous electrolytes are an appropriate choice for focus when choosing a potential MAB for grid-scale energy storage system.

4. Iron as an Alternative Anode – A Fertile Ground for Research

With everything stated so far in regards the given alternatives and their status, Fe anodes are a reviving niche of MABs, which recently regained the interests of researchers.^[80–82] A schematic representation of the iron-air cell can be seen in Figure 4, illustrating the typical redox processes on both electrodes. Just

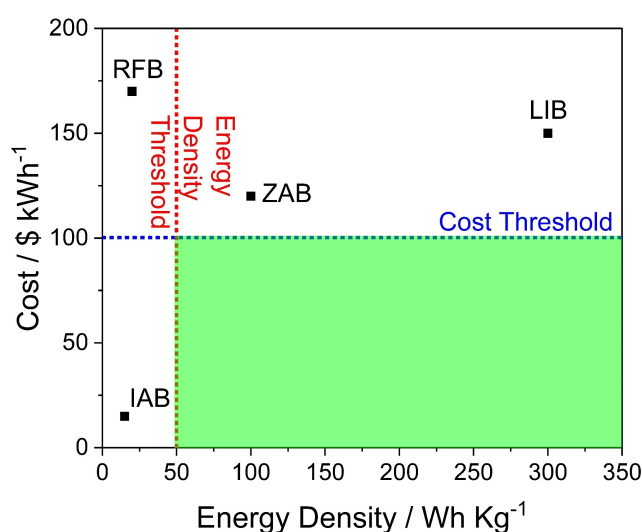


Figure 3. Cost and energy density thresholds according to,^[3] LIB,^[3,76,77] FRB,^[3,5,34] MABs (IAB, ZAB).^[75]

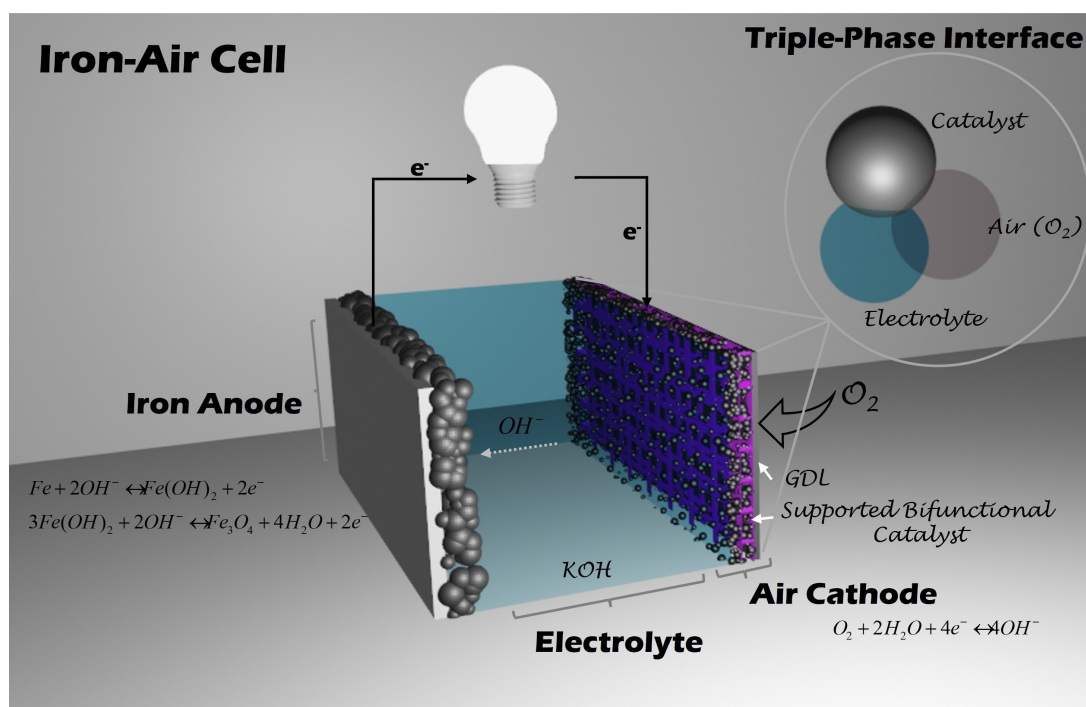


Figure 4. A schematic illustration of an iron-air cell, including magnification of the triple-phase interface in the air-cathode.

as Zn, it serves as an anode in typical “old school” battery chemistries.^[83,84] It is non-toxic, inexpensive, has low price volatility, recyclable and exhibits multielectron redox activity. Additionally, compared to Zn, it has a rich valency state range, much more abundant in the earth crust (47,000 ppm compared to 83 ppm), much cheaper (120 \$ton⁻¹ compared to 2550 \$ton⁻¹), has relatively higher theoretical gravimetric (960 mAh g⁻¹ compared to 820 mAh g⁻¹) and volumetric (7557 mAh cm⁻³ compared to 5851 mAh cm⁻³) capacity^[83,85] (Figure 2a). Parametrically, the notable drawback is the difference in battery voltage (1.26 V compared to 1.66 V), resulting in lower specific energy when oxygen intake is being included (763 Wh Kg⁻¹ versus 1090 Wh Kg⁻¹)^[39,43] (Figure 2b).

These values attract and spark the enthusiasm not only of individual researchers in the framework of academic institutions, but also government funded platforms globally (for example: European Battery Alliance in the EU,^[75] the UK government,^[86,87] Germany,^[88] Israel^[89] (Israel National Institute for Energy Storage)), and even pioneering companies (Form Energy, the US).^[90] The latter illustrates the same idea that was reported by CETO (JRC) in 2023, according to which iron-air batteries are technologically mature enough to stand side-by-side with Zn-air batteries (TRL 6–7), while Li-, Al-, and Mg-air batteries are falling behind (TRL ≤ 5).^[75] On this note, the practical aspects associated with employing iron as an alternative vary and include sustainability, state-of-the-art performance and intrinsic challenges.

First, in this context, one should consider sustainability in terms of emissions in the production phase and recyclability as these stages have a major impact on the global warming potential. For the sake of simplicity, the major elements

associated with the active material in chosen MABs, namely lithium, zinc, and iron, will be considered as the sole anode material in order to highlight the relative impact on the carbon footprint. Let us start with Li: it is derived from brine or ores,^[91] and these two routes vary tremendously. Whereas brine is sequentially evaporated to produce a concentrate, lithium ore is extracted, crushed and milled before being cyclically floated to acquire the concentrate.^[92,93] The former has far lower impact, contributing around 0.2 g CO₂ eq/t of Li brine, whilst the latter provides 0.4 t CO₂ eq/t of Li ore.^[92] In general, brine utilization pathways is less energy consuming process, as this pathway partially relies on solar energy, while ore processing requires the utilization of fossil fuels, as an energy source. Next, concentrates of both brine and ore, are further processed to produce lithium carbonate and lithium hydroxide. These processes produce about 20 t CO₂ eq/t of Li products.^[92] Whereas, rolled lithium metal produced via electrolysis from LiCl-KCl eutectic molten salt solution, extrusion and rolling is estimated to produce a total carbon footprint of 50 t CO₂ eq/t of Rolled Li^[94] and in other case studies, it is estimated to be as high as 167–170 t CO₂ eq/t of Li.^[95,96]

On the other hand, zinc and iron are both extracted from ore and the process of smelting is dominant in the production of both metals. It is considered rather simple and less environmentally demanding, in comparison to lithium. For instance, zinc production requires 2.6–6.6 t CO₂ eq/t of Zn.^[16,97–99] Iron mining, processing and pelletizing is even less consuming and stands at about 0.02–0.26 t CO₂ eq/t of Fe.^[100–103] This rather large difference is a straight outcome of the common zinc versus iron natural mineralogical occurrence, which necessitates additional separation.^[98,104] At the other end of the battery cycle life there

is the recycling stage, which is not only essential to sustaining a favorable climate, but it also provides an opportunity to establish a circular economy, reducing production emissions and reliance on the raw material supply chain.^[105] Iron and its alloys are common engineering products used in transportation, construction, and industrial applications.^[106]

In terms of recycling, the end-of-life recovery rate of iron is the highest and it stands on >60%, while for zinc it is only about 40–50% and for lithium it is less than 5%.^[82,107,108] Moreover, the impact of secondary zinc and iron production on carbon footprint reduction is estimated to be 40% and 60%,^[109] respectively. This information likewise includes a hidden and unfortunate fact, which should be addressed in the advent of iron implementation in emerging energy application. The low price and wide abundance possess a double-edged sword; while they encourage active production, given the current annual production volume of iron and steel industry, they also account for a quarter of global industrial emissions and 6% of global energy consumption.^[82,107] This means that production should be regulated to minimize the environmental impact. Production from virgin iron ore requires at least tenfold cumulative energy input compared to production from scraps,^[110] but it is currently less expensive.^[111] Thus, significant efforts are dedicated to reduce carbon emissions through alternative, more sustainable iron manufacturing technologies.^[82]

On this basis, innovative battery concepts based on iron would hopefully promote development in the production and recycling processes, thereby supporting global shift from fossil fuel-based production mode to greener concepts. Some of these concepts rely on hydrogen as a reducing agent, like direct reduced iron (DRI)^[82] (while DRI for example is claimed to be employed as the raw material of the anodes by Form Energy in their official website^[112]). DRI is industrially mature and making progress in actual commercialization (current DRI production is estimated to be about 8% and will reach 17% by 2030, according to the international energy agency^[113]). Coal-based DRI is estimated to reduce the CO₂ emissions by 38%.^[82,114] This decrease cannot be dissociated from the significantly higher price (>20%).^[115,116] Additional disadvantages still remain, such as dependence on costly green hydrogen and a relatively lower quality of iron oxide output.^[82] A thorough review considering the progress and challenges of DRI can be found in Yang and Tian et al^[114] review.

Other alternatives, which are more promising in CO₂ reduction (>90%), currently either have low energy efficiency, like hydrogen plasma smelting reduction, electrowinning, and molten oxide electrolysis, or require further investigation and scaling, like deep eutectic solvent extraction. These aspects are comprehensively discussed in Luin et al review.^[82] An additional aspect for sustainability is abundance, or more realistically, the relative availability based on the reserves to resource ratio, and the fact that iron is not considered a critical raw material as opposed to lithium, magnesium and even zinc, both by the EU^[69] and the US.^[70] World resources of iron are estimated to be about 230 billion tons of iron, while the reserves are about 37%. To emphasize this data, for zinc and lithium, for example

world resources are estimated to be 1.9 billion and 105 million tons, while the reserves are 11% and 26% correspondingly.^[70]

Second, in terms of practical performance, cutting-edge iron-air MABs are inadequate to deliver the theoretical metrics. The coulombic efficiency is generally low. While rechargeable batteries are usually having the benefit of relatively high coulombic efficiency, i.e. 85–95%, iron-air batteries suffer from nearly 60%.^[81]

Nevertheless, it is worth noting that the iron anode in this couple is not necessarily the only bottleneck, as some iron anodes in aqueous alkaline medium, enable cycling under a restricted depth of discharge, obtaining higher coulombic efficiency but compromising cycle life to some extent, withstanding still many cycles.^[83,84,117] Whereas this fact highlights that iron chemistry is currently incapable of supporting deep discharge with long cycling endurance,^[80,118] which would allow for greater utilization while minimizing volume. The fundamental underlying processes compromising iron anode performance may be roughly classified as passivation,^[43,80,83,119] irreversible passive phases accumulation,^[80,119] HER during charging,^[43,83,119,120] corrosion,^[43,119] intrinsic mechanical instabilities related to the reaction mechanism during cycling and irreversible morphological transformation.^[80,121] The multistep discharge process inevitably is based on a complex mechanism, combining both chemical and electrochemical reactions, resulting in the formation of hydroxides, oxyhydroxides and oxides. The formed products are less conductive than the active elemental iron, and by covering the metal surface they passivate it, forming a barrier with high charge transfer resistance. These products are naturally more voluminous compared to iron, thus increasing internal stress and particle pulverization.

Undesired phases, including γ -Fe₂O₃ (maghemite), often tend to accumulate irreversibly and via gradual reduction of active surface, capacity fades till failure.^[83] Following pulverization, the previously described gradual accumulation causes loss of physical contact between the particles, and in addition the loss of contact between the particles and the binder, resulting in poor adhesion, and pore blockage, which forms a diffusion barrier for the electrolyte; this would eventually result in additional capacity loss as the utilization of the active mass drops. Given the remaining exposed active surface determines the cycle number to failure,^[122] active material utilization depends on wetting and the accessibility and therefore, introducing sufficient porosity to the structure of the anode may improve the utilization.^[123]

Capacity loss can also be induced by corrosion process, upon which hydrogen gas evolved, resulting in considerable self-discharge, apparent as shorter shelf life with a scope of 20% capacity loss within 14 days.^[43,81,83] Parasitic HER also reduces the faradaic efficiency regardless of the transient electrode surface condition during cycling.^[120] This process is especially evident during the formation cycles, when morphological changes result in a surface area increase, dictating electrode potential-dependent gas evolution intensity, with the same faradaic loss recorded at relatively positive potentials. This issue may somewhat be mitigated if a charging cut-off is set up,

limiting the oxidation up to the two-electron step, thus reducing the extent of irreversible passivation;^[121] nevertheless, this avenue reduces the voltage and, indirectly, it would mean that the energy density is compromised, as well (Table 1 demonstrates these challenges).

Comprehensively, while Zn and Fe based anodes grow dendrites in mild and acidic mediums, and the former also in alkaline mediums,^[124–126] and given that they all rely on the dissolution-deposition mechanism, Fe based anodes in alkaline medium operate by conversion, which has the advantage of being free of this phenomenon.^[83] As a result, unlike Zn, it is less likely to lose active material along the charging phase of cycling, and shorts are less likely.

Given the reasonably thorough analysis of the obstacles, a realistic perspective should also be presented. These challenges are managed by modifying the chemical composition of the electrolyte or the electrode or via a focus on the electrode structure. The first strategy focuses on selectively enhancing the overpotential of HER in order to slow its rate in relation to the reversible iron conversion. The common go-to electrolyte and electrode additives are based on bismuth and sulfide salts, among which are Bi_2O_3 , Na_2S , K_2S , Bi_2S_3 , and FeS .^[43,83,119,127,128] Metallic bismuth deposit obtained during the process of charging acts as a site with an increased HER overpotential. Indium salts are another type of additive that is similar to bismuth-based ones.^[129] Inorganic sulfide species role is mainly via imparting de-passivation conditions, since the sulfide of iron conductivity is greater than that of iron hydroxide/oxide. Linear and cyclic organosulfur-based additives reduce HER by covering the surface via adsorption, allowing for both HER reduction and efficient corrosion inhibition.^[83,130,131] Other chalcogenide-based additives, such as selenide, are a recent addition to the additive pool. Tomar et al.^[132] recently demonstrated that electrodes incorporating FeSe in their formulation or electrolytes containing selenates are capable of superior cycling performance and reduced capacity loss when compared to sulfide-based additives. Furthermore, the additive's uniqueness is its regeneration capacity, a property that sulfide lacks during cycling. Another common additive is LiOH , which is believed to actively change the conversion process, enhancing charging efficiency and reversibility via intercalation.^[83,133]

Structural modification on the other hand, is achieved by increasing the active surface area, which is raised from nearly the geometrical area of the bulk to a much larger area, dictated by the nanostructure of particles, changing the electrode preparation method, or using different binder and pore-formers.^[134] Another approach involving structural and chemical modification is compositing the active material particles to maintain mechanical stability and integrity, while minimizing surface deactivation during cycling. For example, many researchers choose carbonaceous confinement, as this approach yields increased conductivity that improves the discharge capacity, maintaining structural integrity as iron dissolution is suppressed and, in some cases, mitigates HER.^[129,135,136] This approach is valid since carbon, as an additive not only improves the conductivity but also eliminates failure due to morphological evolution,^[43,133] a mechanism that underpins capacity fading

as described by Lee et al.^[121] Others provide structural integrity by using various binders^[137,138] to ensure the cohesion of particles in pressed, casted, and impregnated electrodes, which tend to provide more active surface than standard sheet-like electrodes due to inherent porosity and the ability to manipulate performance combined with electrode additives. In this context, sintering, as an electrode preparation method, provides better electrical contact with controllable porosity distribution and size, resulting in the largest active surface area; however, there is no ability to improve performance further with electrode additives, thus in this case, researchers must rely solely on electrolyte additives.^[43]

Iron-air batteries based on solid and quasi-solid electrolytes have been also studied. These batteries offer a relatively high energy density (high capacity^[154] and, in certain circumstances, $V > 1$ ^[153]), minimal self-discharge as compared to low-temperature iron-air batteries, and the ability to operate using waste heat, which in sustainability aspect is efficient. Under the category of solid-state electrolyte, there are two common configurations.^[155] The first which is more mature, is the solid oxide iron-air redox battery. Proper charging of this configuration depends on the $\text{H}_2/\text{H}_2\text{O}$ redox couple mediator via water electrolysis. In this system, the iron oxide actually serves as a mediator that operates in a separate storage unit, while the cell itself is a solid oxide fuel cell. In that manner, the poor reaction kinetics caused by buildup of passive products from deeply discharged iron anodes may be avoided since volume expansion^[121,129,152] of the active material is decoupled in this unique design, as demonstrated by Tang et al.^[152,155] The second type, the all-solid-state iron-air battery, is simpler, matches typical battery configuration, and does not require a mediator. These simpler designs operate at high temperature and is based on solid-state redox pathways.^[156] They demonstrate consistent and promising performance, with coulombic efficiency over 80% for hundreds of cycles.^[153] Unlike traditional room-temperature liquid electrolytes-based iron-air cells, their performance is less affected by minor temperature fluctuations, while the self-discharge is neglectable.^[155] The insignificant capacity loss during cycling is due to coarsening of iron particles during cycling,^[153] rather than irreversible passivation accumulation.

The electrolytes used in both types often have lower conductivity and are more expensive than aqueous electrolytes since specialty powder mixes for electrode preparation and thermal processing such as annealing and sintering are required. Furthermore, operation demands high temperatures (500–800 °C) to activate the diffusivity of O^{2-} across the electrolytic matrix, which essentially reduces the roundtrip efficiency.^[157] On the other hand, it is noteworthy that safety issues like thermal runaway, which LIBs exhibit through dendrite growth and shortening, are addressed, and, unlike aqueous batteries, where HER is a major difficulty to tackle, no pressure buildup or leakage is feasible.

Conversely, sustainability and end-of-life disposal should also be considered, despite the prematurity to enter the market. Jacob et al.^[158] evaluated typical recycling procedures for LIBs as were applied to solid state electrolytes. Pyrometallurgy is claimed to be less suitable in this scenario since the process

Table 1. Overview of selected Fe-based anodes and their performance.

Active Material	Electrolyte	Potential Range	Specific Capacity	Capacity Retention	Coulombic efficiency (1 st cycle)	Ref.
α -Fe ₂ O ₃ in N-doped carbon hollow nanowall arrays directly grown on carbon textiles	3 M KOH	−1.4–0 V vs. Ag/AgCl	130 mAh cm ^{−2} at 30 mA cm ^{−2}	81.9% after 5000 cycles at 30 mA cm ^{−2}	104% at 30 mA cm ^{−2}	[139]
Fe ₃ O ₄ /MoS ₂ /NIS composite	6 M KOH + 0.6 M LiOH	−1.25–−0.4 V vs Hg/HgO	637.9 mAh g ^{−1} at 0.6 A g ^{−1} 442.1 mAh g ^{−1} at 2.4 A g ^{−1}	88.5% after 100 cycles at 0.3 A g ^{−1} 78.6% after 100 cycles at 2.4 A g ^{−1}	~83% at 0.6 A g ^{−1}	[140]
Fe ₃ O ₄ nanoparticles on 3D oxygen functionalized graphite	6 M KOH	−1.25 V–−0.4 V vs Hg/HgO	634 mAh g ^{−1} at 5 A g ^{−1} 504 mAh g ^{−1} at 100 A g ^{−1}	79% after 2000 cycles at 5 A g ^{−1}	95% at 5 A g ^{−1} 99% at 100 A g ^{−1}	[141]
FeO _x -dominated composite aerogel	6 M KOH + 0.5 M LiOH + 0.05 M Na ₂ S	−1.2 V–−0.4 V vs SCE	470 mAh g ^{−1} at 0.5 A g ^{−1} 230 mAh g ^{−1} at 5 A g ^{−1}	97.8% after 120 cycles at 1 A g ^{−1}	90% at 1 A g ^{−1}	[142]
Fe ₃ O ₄ + 10 wt% S	6 M KOH + 15 g L ^{−1} LiOH	−1.2 V–−0.4 V vs Hg/HgO	430 mAh g ^{−1} at 5 C	96.4% after 100 cycles at 2 C/5 C	62.8% at 2 C/5 C	[143]
Core-shell structured C-Fe	1 M KOH	−1.2 V–−0 V vs SCE	208 mAh g ^{−1} at 1 A g ^{−1}	93% after 2000 cycles at 4 A g ^{−1}	~90% at 4 A g ^{−1}	[135]
Pressed-Plate Carbonyl Iron + 8.5 wt% Bi ₂ S ₃	6 M KOH	−1.7 V–−0.75 V vs SCE	188 mAh g ^{−1} at 20 mA	-	94% at 20 mA	[120]
Fe ₃ O ₄ /C-Bi composites	6 M KOH + 15 g/L LiOH + 0.1% Na ₂ S	−1.2 V–−0.4 V vs Hg/HgO	700 mAh g ^{−1} at 300 mA g ^{−1}	90% after 100 cycles at 300 mA g ^{−1}	95.2% at 300 mA g ^{−1}	[144]
Carbonyl iron + 5 wt% FeSe	30 w/v %	−1.2 V–+0.6 V vs Hg/HgO	220 mAh g ^{−1} at C/2	96% after 2000 cycles at C/2	85% at C/2	[132]
S-modified Fe ₂ O ₃	6 M KOH	−1.25 V–−0.55 V vs Hg/HgO	400 mAh g ^{−1} at 0.2 C	65% after 100 cycles at 0.2 C	50% at C/2	[145]
S-modified Fe ₂ O ₃	6 M KOH	−1.2 V–−0.4 V vs Hg/HgO	500 mAh g ^{−1} at 0.2 C	74% after 100 cycles at 0.2 C	98.5% at 0.2 C	[80]
Fe ₂ O ₃ /C composite	8 M KOH + 0.01 M K ₂ S	−1.3 V–−0.1 V vs Hg/HgO	425 mAh g ^{−1} at 0.5 mA cm ^{−2} 825 mAh g ^{−1} at 50 mA cm ^{−2}	93% after 30 cycles at 0.5 mA cm ^{−2} 55% after 30 cycles at 50 mA cm ^{−2}	45% at 0.5 mA cm ^{−2} 81% at 50 mA cm ^{−2}	[127]
Carbonyl iron + 5w/w% ZnS	30 w/v %	−1.35 V–−0.75 V vs Hg/HgO	326 mAh g ^{−1} at C/2 rate	99% after 750 cycles at C/2	95% at C/2	[146]

induces cross-reactions as well as complex redistribution of elements in the electrolyte matrix, and requires high energy input and additional mineral resources for sufficient recovery; hence, hydrometallurgy and direct recycling seem more attainable. Yet, the recovery via these procedures entails prior strategizing since the dissolution and synthesis chemistries necessitate particular approaches per different electrolyte classes, considering more complex schemes as the multiplicity of constituent elements is prominent.^[158,159]

Overall, iron-air batter technologies meet the requirements of grid-scale energy storage in terms of cost-efficiency, diversity in operation conditions, safety, sustainability and scalability, putting them in a relatively high position when considering the technological readiness for production. However, performance should be further optimized as they still do not meet the benchmark performance for grid energy storage. The key challenge that remains is utilization of the active material to deliver adequate energy density over long cycling.

5. The Air-Cathode: Rate and Cycling Determining Factor

Nonetheless, considering everything discussed in the previous paragraphs, the hidden limiting factor is actually not the iron anode, which is considered relatively robust in comparison to the air cathode (about threefold more).^[81] Although this perspective spotlights iron as a viable alternative, challenges associated with this component are not to be overlooked and will certainly be discussed briefly in this paragraph. The cathode requires a three-phase region: a solid conductive electrode to transfer electrons, a porous structure for oxygen diffusion, and an electrolyte to sustain the reaction and product migration.^[40,41] The oxygen reduction reaction can occur via two pathways: the desired four-electron pathway or the less desirable two-electron pathway, which results in the formation of peroxo species, a strong oxidizing entity.^[160] Thus, ORR catalysts must exhibit high selectivity toward the four-electron pathway. The key to this selectivity is the direct bond breaking of oxygen. The reversible oxygen evolution reaction via a four-electron pathway is both kinetically and thermodynamically demanding due to the formation of O–O and O–H bonds. These requirements mandate a bifunctional character on the catalyst, which must reduce overpotentials for both ORR and OER to reduce efficiency loss while remaining stable during cycling.^[81] Currently, bifunctionality is accomplished through the combination of two separate catalysts that address each reaction separately, thereby compromising the number of active sites, or by the selection of single catalysts that improve both to some extent.^[161] The best performing and stable catalysts are based on the combination of noble metals (for ORR) and their oxides (for OER);^[160] however, since they are considered critical raw materials^[69] and are extremely expensive,^[162] scaling these air electrodes for grids is economically impracticable. Hence, some cheaper alternatives are

studied, such as transition metal-based compound, i.e. oxides, phosphates, sulfides and phosphides.^[160]

In this context, the most prevalent non-noble alternatives are based on mixture of carbonaceous species with transition metal oxides.^[160,163] While carbon contributes to the catalytic first step of the ORR, i.e. reduction of oxygen to peroxide, the transition metal oxide is responsible for peroxide breakdown via disproportionation. Such metal oxides are commonly MnO₂ and Co₃O₄. These catalysts are affordable; however, the first has better ORR activity, whereas the latter has primarily OER activity, and both have low conductivity, and necessitate additional manipulations to modify the catalytic activity, such as doping and defect engineering, which change the activity via change in the electronic structure, and morphology or crystalline nature changes.^[164] The combination with carbonaceous species offers not only the aforementioned catalytic enhancement but also a supporting scaffold. Nonetheless, they deteriorate gradually given their poor oxidation stability, leading to capacity fading and structural integrity loss, which causes flooding.^[165] Carbonates formed during carbon oxidation or reaction with atmospheric carbon dioxide from untreated feed can cause electrolyte acidification, trigger precipitation that blocks further diffusion of electrolyte and oxygen to the triple-phase interface.^[66,81,166] To tackle the stability issue, carbonaceous supports and catalysts with increased degree of graphitization are employed, e.g. carbon nanotubes, multilayer graphene and mesoporous carbon.^[167] While all provide with higher surface area and stability, the first two additionally benefit via their two-dimensional nature, which allows to improve the contact with the supported additional catalyst via basal and edge sites, lowering electron transfer resistance. The activity of such alternatives can be tailored by functionalization to improve dispersion of co-catalysts,^[168] doping^[169] and increasing the degree of graphitization^[163,167] further with the goal of intensifying the co-catalyst-support interaction.

Tailoring the catalyst's activity or the support's stability is not the only essential matter to bear in mind. In fact, electrode structure is a major barrier to the longevity and the performance of these electrodes. A unique architecture for battery electrode should be provided to ensure optimal performance. In aqueous electrolytes, a three-phase interface (see Figure 4) should be maintained, i.e. the interface between the electrolyte, catalyst and oxygen. To realize such design, a common air electrode has a catalyst layer supported by a current collector and a gas diffusion layer (GDL) facing the gas inlet. All three components must be porous to enable sufficient oxygen transport, and the GDL must be hydrophobic to prevent electrolyte leakage. A balance between hydrophobicity and oxygen transport should be maintained, since both factors are often conflicting, as excessive hydrophobicity would result in flooding, while oxygen has limited solubility in the electrolyte, resulting in inability to stabilize the triple phase interface. The solution to this challenge is to modify the quantity of fluorocarbons added to the GDL, such as PTFE and PVDF.^[66,170]

The current collector is another configurable component that could play a major role in the air cathode performance. It is often a high-surface mechanically robust porous material with

sufficient conductivity, based on metallic foams and meshes or carbonaceous supports. In newer classes of catalysts, researchers attempt to integrate all of the needed properties from the air cathodes with more advanced designs,^[171,172] such as three-dimensional self-standing or directly grown on a support alternatives, e.g. metal organic frameworks and composites.^[173–177]

In practice, the cathode is responsible for energy losses and inferior rate capabilities. For instance, in most of the examples for aqueous iron-air cells displayed in Table 2, the anode's polarization does not surpass 150 mV, although the cathode, according to Timofeeva et al,^[160] has at least 350 mV polarization loss for the ORR (during discharge). These losses result in decreased energy density, which is only around 80% of the theoretical value.

6. Concluding Remarks

To conclude, one needs to look at the unfortunate view regarding the technical feasibility of Fe MABs. Currently, the most likely grid-scale energy storage option for this battery, considering both specific energy and frequency of energy supply, is for grid reliability as a short-term backup power source, i.e. uninterruptible power source (UPS). Other short-term possibilities, such as a black start, are less probable since self-discharge occurs too fast, which makes it unreliable. Long-term energy storage scenarios, like off-grid energy storage or peak shaving are yet out of the question due to insufficiently low specific energy. Nonetheless, this Perspective supports the idea of iron as a viable anode for aqueous MABs rather than a corroding concept; however, more research is needed to be conducted in this rather virgin and unplowed field to qualify and quantify the iron-air battery concept to bring it to stand at high TRL level, side by side with other trending chemistries. To shorten the period of this concept realization, research should be focused on three key routes. The first and second involve tackling the challenges associated with the iron anode and the air cathodes. The third is actually optimization of the operation conditions and ensuring that they serve the long-term operation scenarios of grid-scale energy storage.

Iron anode performance optimization includes four strategies. First, mitigating corrosion process via the utilization of inexpensive and environmentally friendly corrosion inhibitors to eliminate self-discharge or electrode/electrolyte interface modification. Second, electrode and electrolyte additives should be employed to assist with selective offsetting of HER onset to increase the charging efficiency. Third, the depth of discharge should be extended without compromising on reversibility utilizing additive and employing mechanistic approaches to highlight the processes that enhance surface activity with less passive phase accumulation. Fourth, employing advanced architectures to substantially enhance the available active surface or to reduce active mass loss.

Air cathode performance optimization includes screening and development of novel cost-effective bifunctional catalysts for the air electrode. This goal can be achieved by addressing

Table 2. Overview of full-cell Fe-air batteries and their performance.

Electrolyte type	Active Materials	Electrolyte	Voltage	Specific Capacity	Capacity retention/Round-trip Efficiency	Coulombic Efficiency (1 st cycle)	Ref.
aqueous	Fe ₃ O ₄ -Pt/C	8 M KOH + 0.03 M K ₂ S	0.8 V	460 mAh g ⁻¹ at 10 mA cm ⁻²	22% after 20 cycles at 10 mA cm ⁻²	~76% at 10 mA cm ⁻²	[147]
	Carbonyl iron + MoS ₂ -Ag/Gr	6 M KOH + 2 mM Na ₂ S	–	299 mAh g ⁻¹ at 50 mA cm ⁻²	97% after 800 cycles at 50 mA cm ⁻²	90% at 50 mA cm ⁻²	[148]
	Fe ₃ O ₄ -embedded rGO composite – Pt/C	8 M KOH + 0.01 M Na ₂ S	0.6 V	420 mAh g ⁻¹ at 1 mA cm ⁻²	100% after 30 cycles at 1 mA cm ⁻²	23% at 1 mA cm ⁻²	[149]
	Fe-Ag/C	6 M KOH + 1 mM EML	–	416 mAh g ⁻¹ at C/5 rate	94% after 1000 cycles at C/5	–	[150]
	Fe nanoparticle-encapsulated C–N composite – Pt/C + IrO ₂	6 M KOH	0.7–1.1 V	–	Failure after 45 cycles at 0.2 mA cm ⁻²	–	[151]
Solid	Fe ₂ O ₃ -BaZr _{0.4} Ce _{0.4} Y _{0.1} O ₃ -IrO ₂	0.5 M K ₂ SO ₄	~1.4 V	–	Stable over 180 cycles	48.4% at 0.2 mA cm ⁻² 22.2% at 2 mA cm ⁻²	[152]
	Fe ₃ O ₄ -Pt/C	(Sc ₂ O ₃) _{0.1} (CeO ₂) _{0.9} (ZrO ₂) _{0.89} At 550 °C KOH–ZrO ₂ at 20 °C, 60% R.H.	1 V	~65 mAh g ⁻¹ at 0.2 C	RTE- 90% at 0.2 C (500 cycles)	–	[147]
	Fe ₂ O ₃ -C _{0.8} Gd _{0.2} O ₂ -La _{0.6} Sr _{0.4} Fe _{0.8} Co _{0.2} O ₃	La _{0.8} Sr _{0.2} Ga _{0.8} Mg _{0.2} O ₃ At 650 °C	0.8 V	70 mAh g ⁻¹ at 0.2 mA cm ⁻²	45% after 20 cycles at 0.2 mA cm ⁻²	87% at 0.2 mA cm ⁻²	[153]
	Fe ₂ O ₃ -C _{0.8} Gd _{0.2} O ₂ -La _{0.6} Sr _{0.4} Fe _{0.8} Co _{0.2} O ₃	La _{0.8} Sr _{0.2} Ga _{0.8} Mg _{0.2} O ₃ At 650 °C	~1 V	508 mAh g ⁻¹ at 1.4 A g ⁻¹	RTE- 53.7% at 1.4 A g ⁻¹ (100 cycles)	80% at 1.4 A g ⁻¹	[153]

the composite nature of the electrode and tuning the morphology of the supported catalysts, allocating alternative stable (chemically and mechanically) supporting materials, or by stabilization of the three-phase zone to allow facile electron transfer and continuous oxygen transport, which can be tuned by the preparation method, changing the nature of the electrical contact or via controlling the wetting and solubility behavior.

The third route is targeting to optimize the operation conditions to meet the required scenario. The dynamic nature of renewable sources requires a framework with minimal and maximal expected performance. In this aspect, electrode design is highly critical when expecting the scaled electrode to deliver matching performance to the lab-scale isolated electrode; it must account for feed, heat losses, electrical contact, and wetting, as well as for an exposure to different climates and environment conditions (min and max operational temperatures windows, relative humidity, amount of air born micro particles (dust) and CO₂ ingress).

Generally, a complex battery system like this one calls for systematic approach and the initiative for collaboration. Despite being in the same field of applied electrochemistry, catalysis research and energy storage research are frequently conducted by different research groups, which reflects the industry's advantage in promoting such technologies. Nevertheless, this is an excellent motivator to make this concept a practical, affordable and realistic solution for grid-scale energy storage in the coming years.

Acknowledgements

The authors would like to thank the Israel Science Foundation (ISF) for the financial support in the frame of project No. 1335/24, and the Israel National Institute for Energy Storage (INIES) and the Nancy & Stephan Grand Technion Energy Program (GTEP) for the vast infrastructure support.

Conflict of Interests

The authors declare no conflict of interest.

Data Availability Statement

The data that support the findings of this study are available from the corresponding author upon reasonable request.

Keywords: Iron-Air Batteries · Grid-Scale Energy Storage · LIBs Alternatives · Sustainability · Multivalent Metal Anodes

- [1] Y. E. Durmus, H. Zhang, F. Baakes, G. Desmaizieres, H. Hayun, L. Yang, M. Kolek, V. Küpers, J. Janek, D. Mandler, S. Passerini, Y. Ein-Eli, *Adv. Energy Mater.* **2020**, *10*, 2000089.
- [2] S. B. Wali, M. A. Hannan, P. J. Ker, S. A. Rahman, K. N. Le, R. A. Begum, S. K. Tiong, T. M. I. Mahlia, *J. Energy Storage* **2024**, *77*, 109986.

- [3] Z. Zhu, T. Jiang, M. Ali, Y. Meng, Y. Jin, Y. Cui, W. Chen, *Chem. Rev.* **2022**, *122*, 16610–16751.
- [4] R. Dmello, J. D. Milshtein, F. R. Brushett, K. C. Smith, *J. Power Sources* **2016**, *330*, 261–272.
- [5] L. Tang, P. Leung, M. R. Mohamed, Q. Xu, S. Dai, X. Zhu, C. Flox, A. A. Shah, Q. Liao, *Electrochim. Acta* **2023**, *437*, 141460.
- [6] "Batteries Europe – Overview of International R&D&I Battery Funding and Global Benchmarks for Battery KPIs, June 2024," can be found under <https://batterieseurope.eu/wp-content/uploads/2024/07/Overview-of-International-RDI-Battery-Funding-and-Global-Benchmarks-for-Battery-KPIs-June-2024pdf.pdf>, n.d.
- [7] "Battery 2030+ Inventing the Sustainable Batteries of the Future: Research Needs and Future Actions, Updated ver. August 2023," can be found under <https://battery2030.eu/wp-content/uploads/2023/09/B-2030-Science-Innovation-Roadmap-updated-August-2023pdf.pdf>, n.d.
- [8] "Batteries Europe – Research and Innovation Roadmap on Battery Technologies: Powering Europe's Green Revolution: Paving the Way to a More Resilient and Sustainable Battery Industry," can be found under https://batterieseurope.eu/wp-content/uploads/2023/09/Batteries-Europe-Research-and-Innovation-Roadmap-2023_pdf.pdf, n.d.
- [9] H. Bae, Y. Kim, *Mater. Adv.* **2021**, *2*, 3234–3250.
- [10] T. Watari, B. McLellan, S. Ogata, T. Tezuka, *Minerals* **2018**, *8*, 156.
- [11] Y. Cao, M. Li, J. Lu, J. Liu, K. Amine, *Nat. Nanotechnol.* **2019**, *14*, 200–207.
- [12] M. Obi, S. M. Jensen, J. B. Ferris, R. B. Bass, *Renewable Sustainable Energy Rev.* **2017**, *67*, 908–920.
- [13] M. A. Pellow, H. Ambrose, D. Mulvaney, R. Betita, S. Shaw, *Sustainable Mater. Technol.* **2020**, *23*, e00120.
- [14] Z. Chen, A. Yildizbasi, Y. Wang, J. Sarkis, *Global Challenge* **2022**, *6*, 2200049.
- [15] Y. Huang, J. Li, *Adv. Energy Mater.* **2022**, *12*, 2202197.
- [16] F. Santos, A. Urbina, J. Abad, R. López, C. Toledo, A. J. Fernández Romero, *Chemosphere* **2020**, *250*, 126273.
- [17] Y. Jiao, D. Månsson, *J. Energy Storage* **2023**, *57*, 106167.
- [18] M. Baumann, J. F. Peters, M. Weil, A. Grunwald, *Energy Technol.* **2017**, *5*, 1071–1083.
- [19] H. Zhou, Y. Yang, W. Li, J. McKechnie, S. Thiede, P. Wang, *One Earth* **2024**, *7*, 1288–1300.
- [20] U. Saleem, B. Joshi, S. Bandyopadhyay, *J. Sustainable Metall.* **2023**, *9*, 950–971.
- [21] J. O. G. Posada, A. J. R. Rennie, S. P. Villar, V. L. Martins, J. Marinaccio, A. Barnes, C. F. Glover, D. A. Worsley, P. J. Hall, *Renewable Sustainable Energy Rev.* **2017**, *68*, 1174–1182.
- [22] R. K. Emmett, M. E. Roberts, *J. Power Sources* **2021**, *506*, 230087.
- [23] P. A. García-Salaberri, in *Nanostructured Materials Engineering and Characterization for Battery Applications*, Elsevier, **2024**, pp. 465–489.
- [24] L. F. Arenas, C. Ponce de León, F. C. Walsh, *Curr. Opin. Electrochem.* **2019**, *16*, 117–126.
- [25] C. Zhang, Z. Yuan, X. Li, *ACS Energy Lett.* **2024**, *9*, 3456–3473.
- [26] J. L. Barton, J. D. Milshtein, J. J. Hinricher, F. R. Brushett, *J. Power Sources* **2018**, *399*, 133–143.
- [27] G. Qiu, C. R. Dennison, K. W. Knehr, E. C. Kumbur, Y. Sun, *J. Power Sources* **2012**, *219*, 223–234.
- [28] Z. Huang, A. Mu, L. Wu, H. Wang, *J. Energy Storage* **2022**, *45*, 103526.
- [29] L. Cao, M. Skyllas-Kazacos, C. Menictas, J. Noack, *J. Energy Chem.* **2018**, *27*, 1269–1291.
- [30] W. Tian, H. Du, J. Wang, J. J. Weigand, J. Qi, S. Wang, L. Li, *Materials* **2023**, *16*, 4582.
- [31] C. A. Machado, G. O. Brown, R. Yang, T. E. Hopkins, J. G. Pribyl, T. H. Epps, *ACS Energy Lett.* **2021**, *6*, 158–176.
- [32] C. H. L. Tempelman, J. F. Jacobs, R. M. Balzer, V. Degirmenci, *J. Energy Storage* **2020**, *32*, 101754.
- [33] B. G. Thiam, S. Vaudreuil, *J. Electrochem. Soc.* **2021**, *168*, 070553.
- [34] S. Ebner, S. Spirk, T. Stern, C. Mair-Bauernfeind, *ChemSusChem* **2023**, *16*, e202201818.
- [35] A. Adeniran, A. Bates, N. Schuppert, A. Menon, S. Park, *J. Energy Storage* **2022**, *56*, 106000.
- [36] M. L. Perry, J. D. Saraidaridis, R. M. Darling, *Curr. Opin. Electrochem.* **2020**, *21*, 311–318.
- [37] A. G. Olabi, M. A. Allam, M. A. Abdelkareem, T. D. Deepa, A. H. Alami, Q. Abbas, A. Alkhalidi, E. T. Sayed, *Batteries* **2023**, *9*, 409.
- [38] X. Yuan, C. Song, A. Platt, N. Zhao, H. Wang, H. Li, K. Fatih, D. Jang, *Int. J. Energy Res.* **2019**, *43*, e4607.
- [39] T. Li, M. Huang, X. Bai, Y.-X. Wang, *Prog. Nat. Sci.* **2023**, *33*, 151–171.
- [40] L. Yaqoob, T. Noor, N. Iqbal, *J. Energy Storage* **2022**, *56*, 106075.

- [41] Y. Li, J. Lu, *ACS Energy Lett.* **2017**, *2*, 1370–1377.
- [42] L. Aspitarte, C. R. Woodside, *Cell Rep. Sustainability* **2024**, *1*, 100007.
- [43] H. Weinrich, Y. E. Durmus, H. Tempel, H. Kungl, R.-A. Eichel, *Materials* **2019**, *12*, 2134.
- [44] J. Ryu, D. Hong, H.-W. Lee, S. Park, *Nano Res.* **2017**, *10*, 3970–4002.
- [45] D. Linden, T. B. Reddy, *Handbook of Batteries*, McGraw-Hill, **2011**.
- [46] X. Zhang, X.-G. Wang, Z. Xie, Z. Zhou, *Green Energy & Environ.* **2016**, *1*, 4–17.
- [47] C. Zhou, K. Lu, S. Zhou, Y. Liu, W. Fang, Y. Hou, J. Ye, L. Fu, Y. Chen, L. Liu, Y. Wu, *Chem. Commun.* **2022**, *58*, 8014–8024.
- [48] W. Zhang, Y. Huang, Y. Liu, L. Wang, S. Chou, H. Liu, *Adv. Energy Mater.* **2019**, *9*, 1900464.
- [49] L. Nazar, in *Electrochemical Power Sources: Fundamentals, Systems, and Applications*, Elsevier, **2021**, pp. 125–156.
- [50] H. Gao, B. M. Gallant, *Nat. Chem. Rev.* **2020**, *4*, 566–583.
- [51] S. A. Freunberger, Y. Chen, Z. Peng, J. M. Griffin, L. J. Hardwick, F. Bardé, P. Novák, P. G. Bruce, *J. Am. Chem. Soc.* **2011**, *133*, 8040–8047.
- [52] R. Black, S. H. Oh, J.-H. Lee, T. Yim, B. Adams, L. F. Nazar, *J. Am. Chem. Soc.* **2012**, *134*, 2902–2905.
- [53] M. M. Ottakam Thotiyil, S. A. Freunberger, Z. Peng, P. G. Bruce, *J. Am. Chem. Soc.* **2013**, *135*, 494–500.
- [54] A. A. Yaroshevsky, *Geochim. Int.* **2006**, *44*, 48–55.
- [55] W. K. Tan, G. Kawamura, H. Muto, A. Matsuda, in *Sustainable Materials for Next Generation Energy Devices*, Elsevier, **2021**, pp. 59–83.
- [56] A. G. Olabi, E. T. Sayed, T. Wilberforce, A. Jamal, A. H. Alami, K. Elsaid, S. M. A. Rahman, S. K. Shah, M. A. Abdelkareem, *Energies* **2021**, *14*, 7373.
- [57] K. Turcheniuk, D. Bondarev, G. G. Amatucci, G. Yushin, *Mater. Today* **2021**, *42*, 57–72.
- [58] H. Liu, X.-B. Cheng, Z. Jin, R. Zhang, G. Wang, L.-Q. Chen, Q.-B. Liu, J.-Q. Huang, Q. Zhang, *EnergyChem* **2019**, *1*, 100003.
- [59] K. Sada, J. Darga, A. Manthiram, *Adv. Energy Mater.* **2023**, *13*, 2302321.
- [60] Y. Li, Y. Lu, P. Adelhelm, M.-M. Titirici, Y.-S. Hu, *Chem. Soc. Rev.* **2019**, *48*, 4655–4687.
- [61] A. I. Ikeuba, P. C. Iwuji, I.-I. E. Nabuk, O. E. Obono, D. Charlie, A. A. Etim, B. I. Nwabueze, J. Amajama, *J. Solid State Electrochem.* **2024**, *28*, 2999–3025.
- [62] H. Zhang, X. Liu, H. Li, I. Hasa, S. Passerini, *Angew. Chem. Int. Ed.* **2021**, *60*, 598–616.
- [63] L. He, C. Lin, P. Xiong, H. Lin, W. Lai, J. Zhang, F. Xiao, L. Xiao, Q. Qian, Q. Chen, L. Zeng, *Trans. Tianjin Univ.* **2023**, *29*, 321–346.
- [64] Y. Wang, Y. Sun, W. Ren, D. Zhang, Y. Yang, J. Yang, J. Wang, X. Zeng, Y. Nuli, *Energy Mater.* **2022**, *2*, 200024.
- [65] P. Goel, D. Dobhal, R. C. Sharma, *J. Energy Storage* **2020**, *28*, 101287.
- [66] Q. Liu, Z. Pan, E. Wang, L. An, G. Sun, *Energy Storage Mater.* **2020**, *27*, 478–505.
- [67] J. Ryu, M. Park, J. Cho, *Adv. Mater.* **2019**, *31*, 1804784.
- [68] M. Salado, E. Lizundia, *Mater Today Energy* **2022**, *28*, 101064.
- [69] “Study on the critical raw materials for the EU 2023 – Publications Office of the EU,” can be found under <https://op.europa.eu/en/publication-detail/-/publication/57318397-fdd4-11ed-a05c-01aa75e-d71a1#>, n.d.
- [70] Mineral Commodity Summaries 2024. Report in Mineral Commodity Summaries: USGS Numbered Series 2024 (p. 212). U.S. Geological Survey. <http://doi.org/10.3133/mcs2024>.
- [71] S. Hu, Z. Wang, J. Wang, S. Pang, B. Wang, M. Zhu, *Coord. Chem. Rev.* **2024**, *517*, 216045.
- [72] G. Cohn, Y. Ein-Eli, *J. Power Sources* **2010**, *195*, 4963–4970.
- [73] Z. Zhao, X. Fan, J. Ding, W. Hu, C. Zhong, J. Lu, *ACS Energy Lett.* **2019**, *4*, 2259–2270.
- [74] S. S. Shinde, N. K. Wagh, C. H. Lee, D. Kim, S. Kim, H. Um, S. U. Lee, J. Lee, *Adv. Mater.* **2023**, *35*, 2303509.
- [75] “Clean Energy Technology Observatory, Batteries for energy storage in the European Union – Publications Office of the EU,” can be found under <https://op.europa.eu/en/publication-detail/-/publication/57cf5951-9d5d-11ee-b164-01aa75ed71a1/language-en>, n.d.
- [76] “Lithium-Ion Battery Pack Prices Hit Record Low of \$139/kWh | BloombergNEF,” can be found under <https://about.bnef.com/blog/lithium-ion-battery-pack-prices-hit-record-low-of-139-kwh/>, n.d.
- [77] J. Liu, J. Xiao, J. Yang, W. Wang, Y. Shao, P. Liu, M. S. Whittingham, *Next Energy* **2023**, *1*, 100015.
- [78] A. Blakers, M. Stocks, B. Lu, C. Cheng, *Prog. Energy* **2021**, *3*, 022003.
- [79] R. J. Mahfoud, N. F. Alkayem, Y. Zhang, Y. Zheng, Y. Sun, H. H. Alhelou, *Renewable Sustainable Energy Rev.* **2023**, *178*, 113267.
- [80] N. I. Villanueva-Martínez, C. Alegre, J. Rubín, R. McKerracher, C. P. de León, H. A. F. Rodríguez, M. J. Lázaro, *Electrochim. Acta* **2023**, *465*, 142964.
- [81] S. R. Narayanan, G. K. S. Prakash, A. Manohar, B. Yang, S. Malkhandi, A. Kindler, *Solid State Ionics* **2012**, *216*, 105–109.
- [82] A. Oarga-Mulec, U. Luin, M. Valant, *RSC Adv.* **2024**, *14*, 20765–20779.
- [83] Z. He, F. Xiong, S. Tan, X. Yao, C. Zhang, Q. An, *Mater. Today* **2021**, *11*, 100156.
- [84] J. M. E. Abarro, J. N. L. Gavan, D. E. D. Loresca, M. A. A. Ortega, E. A. Esparcia, J. A. D. R. Paragguá, *Batteries* **2023**, *9*, 383.
- [85] X. Wu, A. Markir, Y. Xu, C. Zhang, D. P. Leonard, W. Shin, X. Ji, *Adv. Funct. Mater.* **2019**, *29*, DOI 10.1002/adfm.201900911.
- [86] “UK battery strategy (HTML version) – GOV.UK,” can be found under <https://www.gov.uk/government/publications/uk-battery-strategy/uk-battery-strategy-html-version>, n.d.
- [87] “Health and safety in grid scale electrical energy storage systems (accessible webpage) – GOV.UK,” can be found under <https://www.gov.uk/government/publications/grid-scale-electrical-energy-storage-systems-health-and-safety/health-and-safety-in-grid-scale-electrical-energy-storage-systems-accessible-webpage>, n.d.
- [88] “Publication of the German electricity storage strategy – Interreg Baltic Sea Region,” can be found under <https://interreg-baltic.eu/projects/energy-equilibrium/publication-of-the-german-electricity-storage-strategy/>, n.d.
- [89] “Israel to Set Up National Research Institute for Energy Storage – The Electricity Hub,” can be found under <https://theelectricityhub.com/israel-to-set-up-national-research-institute-for-energy-storage/>, n.d.
- [90] “Form Energy: We are Transforming the Grid,” can be found under <https://formenergy.com/>, n.d.
- [91] U. Wietelmann, R. J. Bauer, in *Ullmann's Encyclopedia of Industrial Chemistry*, Wiley, **2000**.
- [92] J. C. Kelly, M. Wang, Q. Dai, O. Winjobi, *Resour. Conserv. Recycl.* **2021**, *174*, 105762.
- [93] S. Khakmardan, M. Rolinck, F. Cerdas, C. Herrmann, D. Giurco, R. Crawford, W. Li, *Procedia CIRP* **2023**, *116*, 606–611.
- [94] M. Chen-Glasser, A. E. Landis, S. C. DeCaluwe, *J. Energy Storage* **2023**, *60*, 106684.
- [95] M. Zackrisson, K. Fransson, J. Hildenbrand, G. Lampic, C. O'Dwyer, *J. Cleaner Prod.* **2016**, *135*, 299–311.
- [96] L. Wang, J. Hu, Y. Yu, K. Huang, Y. Hu, *J. Cleaner Prod.* **2020**, *276*, 124244.
- [97] X. Xiao, X. Songwen, G. Xueyi, H. Kelong, Y. Ryoichi, *Int. J. Life Cycle Assess.* **2003**, *8*, 151.
- [98] E. Van Genderen, M. Wildnauer, N. Santero, N. Sidi, *Int. J. Life Cycle Assess.* **2016**, *21*, 1580–1593.
- [99] C. Qi, L. Ye, X. Ma, D. Yang, J. Hong, *J. Cleaner Prod.* **2017**, *156*, 451–458.
- [100] T. Norgate, N. Haque, *J. Cleaner Prod.* **2010**, *18*, 266–274.
- [101] N. Haque, T. Norgate, in *Iron Ore*, Elsevier, **2015**, pp. 615–630.
- [102] Y. Gan, W. M. Griffin, *Resour. Policy* **2018**, *58*, 90–96.
- [103] W. Lv, Z. Sun, Z. Su, *J. Cleaner Prod.* **2019**, *233*, 1314–1321.
- [104] R. Stace, in *Iron Ore*, Elsevier, **2022**, pp. 249–268.
- [105] C. Hagelüken, J. Lee-Shin, A. Carpentier, C. Heron, *Recycling* **2016**, *1*, 242–253.
- [106] F. Passarini, L. Ciacci, P. Nuss, S. Manfredi, *Material Flow Analysis of Aluminium, Copper, and Iron in the EU-28*, Publications Office, **2018**.
- [107] P. L. Talens, P. Nuss, F. Mathieux, G. Blengini, *Towards Recycling Indicators Based on EU Flows and Raw Materials System Analysis Data 2018*, (EUR 29435 EN, Publication Office of the European Union-Luxembourg), DOI: 10.2760/092885, JRC112720.
- [108] A. Alessia, B. Alessandro, V.-G. Maria, V.-A. Carlos, B. Francesca, *J. Cleaner Prod.* **2021**, *300*, 126954.
- [109] M. Kaya, S. Hussaini, S. Kursunoglu, *Hydrometallurgy* **2020**, *195*, 105362.
- [110] L. D. D. Harvey, *Renewable Sustainable Energy Rev.* **2021**, *138*, 110553.
- [111] M. R. Gorman, D. A. Dzombak, C. Frischmann, *Resour. Conserv. Recycl.* **2022**, *184*, 106424.
- [112] “Form Energy's Virtual Lab Tour on Vimeo,” can be found under <https://vimeo.com/797119482>, n.d.
- [113] “Tracking Clean Energy Progress 2023 – Analysis – IEA,” can be found under <https://www.iea.org/reports/tracking-clean-energy-progress-2023#overview>, n.d.
- [114] J. Ling, H. Yang, G. Tian, J. Cheng, X. Wang, X. Yu, *J. Cleaner Prod.* **2024**, *441*, 140933.
- [115] D. Gielen, D. Saygin, E. Taibi, J. Birat, *J. Ind. Ecol.* **2020**, *24*, 1113–1125.

- [116] J. Mayer, G. Bachner, K. W. Steininger, *J. Cleaner Prod.* **2019**, *210*, 1517–1533.
- [117] K. Vijayamohan, T. S. Balasubramanian, A. K. Shukla, *J. Power Sources* **1991**, *34*, 269–285.
- [118] H. A. F. Rodriguez, R. D. McKerracher, C. P. de León, F. C. Walsh, *J. Electrochem. Soc.* **2019**, *166*, A107–A117.
- [119] R. D. McKerracher, C. Ponce de Leon, R. G. A. Wills, A. A. Shah, F. C. Walsh, *ChemPlusChem* **2015**, *80*, 323–335.
- [120] H. Weinrich, J. Pleie, B. Schmid, H. Tempel, H. Kungl, R. Eichel, *Batteries & Supercaps* **2022**, *5*, e202100415.
- [121] D.-C. Lee, D. Lei, G. Yushin, *ACS Energy Lett.* **2018**, *3*, 794–801.
- [122] H. Weinrich, M. Gehring, H. Tempel, H. Kungl, R.-A. Eichel, *J. Appl. Electrochem.* **2018**, *48*, 451–462.
- [123] H. Weinrich, M. Gehring, H. Tempel, H. Kungl, R.-A. Eichel, *Electrochim. Acta* **2019**, *314*, 61–71.
- [124] N. Wang, H. Wan, J. Duan, X. Wang, L. Tao, J. Zhang, H. Wang, *Mater. Today* **2021**, *11*, 100149.
- [125] Y. Zuo, K. Wang, P. Pei, M. Wei, X. Liu, Y. Xiao, P. Zhang, *Mater. Today Energy* **2021**, *20*, 100692.
- [126] Y. Zhang, Y. Tian, Z. Wang, C. Wei, C. Liu, Y. An, B. Xi, S. Xiong, J. Feng, *Chem. Eng. J.* **2023**, *458*, 141388.
- [127] B. T. Hang, T. Van Dang, N. Van Quy, *J. Electron. Mater.* **2022**, *51*, 2168–2177.
- [128] J. Jiang, J. Liu, *Interdiscip. Mater.* **2022**, *1*, 116–139.
- [129] D. Lei, D.-C. Lee, E. Zhao, A. Magasinski, H.-R. Jung, G. Berdichevsky, D. Steingart, G. Yushin, *Nano Energy* **2018**, *48*, 170–179.
- [130] S. Malkhandi, B. Yang, A. K. Manohar, G. K. S. Prakash, S. R. Narayanan, *J. Am. Chem. Soc.* **2013**, *135*, 347–353.
- [131] B. Yang, S. Malkhandi, A. K. Manohar, G. K. Surya Prakash, S. R. Narayanan, *Energy Environ. Sci.* **2014**, *7*, 2753.
- [132] Y. Tomar, A. S. Rajan, A. Irshad, D. Mitra, S. R. Narayanan, G. K. S. Prakash, *J. Electrochem. Soc.* **2024**, *171*, 120542.
- [133] B. T. Hang, D. H. Thang, *J. Electroanal. Chem.* **2016**, *762*, 59–65.
- [134] J. Yang, J. Chen, Z. Wang, Z. Wang, Q. Zhang, B. He, T. Zhang, W. Gong, M. Chen, M. Qi, P. Coquet, P. Shum, L. Wei, *ChemElectroChem* **2021**, *8*, 274–290.
- [135] X. Wu, H. Zhang, K.-J. Huang, Z. Chen, *Nano Lett.* **2020**, *20*, 1700–1706.
- [136] E. Shanguan, F. Li, J. Li, Z. Chang, Q. Li, X.-Z. Yuan, H. Wang, *J. Power Sources* **2015**, *291*, 29–39.
- [137] H. Kitamura, L. Zhao, B. T. Hang, S. Okada, J. Yamaki, *J. Power Sources* **2012**, *208*, 391–396.
- [138] T. T. Anh, V. M. Thuan, D. H. Thang, B. T. Hang, *J. Electron. Mater.* **2017**, *46*, 3458–3462.
- [139] W. Li, Q. Xu, D. Kong, H. Yang, T. Xu, H. Wang, J. Zang, S. Huang, X. Li, Y. Wang, *Chem. Eng. J.* **2023**, *452*, 139251.
- [140] H. Tang, M. Liu, L. Kong, X. Wang, Y. Lei, X. Li, Y. Hou, K. Chang, Z. Chang, *Nanomaterials* **2022**, *12*, 3472.
- [141] Z. Qin, Y. Song, H.-Y. Shi, C. Li, D. Guo, X. Sun, X.-X. Liu, *Chem. Eng. J.* **2020**, *400*, 125874.
- [142] T. Huang, W. Liu, Y. Liu, Q. Hou, S. Chen, R. Li, H. Liu, *Next Energy* **2024**, *2*, 100076.
- [143] E. Shanguan, S. Fu, C. Wu, X. Cai, J. Li, Z. Chang, Z. Wang, Q. Li, *Electrochim. Acta* **2019**, *301*, 162–173.
- [144] Z. Sun, L. Kong, X. Wang, Y. Lei, X. Li, H. Tang, Y. Hou, K. Chang, Z. Chang, *Int. J. Hydrogen Energy* **2023**, *48*, 9785–9796.
- [145] N. Villanueva, C. Alegre, J. Rubin, H. A. Figueredo-Rodríguez, R. D. McKerracher, C. P. de León, M. J. Lázaro, *ACS Appl. Energy Mater.* **2022**, *5*, 13439–13451.
- [146] D. Mitra, A. S. Rajan, A. Irshad, S. R. Narayanan, *J. Electrochem. Soc.* **2021**, *168*, 030518.
- [147] W. K. Tan, K. Asami, Y. Maeda, K. Hayashi, G. Kawamura, H. Muto, A. Matsuda, *Appl. Surf. Sci.* **2019**, *486*, 257–264.
- [148] E. O. Aremu, K.-S. Ryu, *Electrochim. Acta* **2019**, *313*, 468–477.
- [149] W. K. Tan, K. Asami, K. Maegawa, R. Kumar, G. Kawamura, H. Muto, A. Matsuda, *Mater. Today Commun.* **2020**, *25*, 101540.
- [150] M. A. Deyab, Q. Mohsen, *Renewable Sustainable Energy Rev.* **2021**, *139*, 110729.
- [151] C. Fang, X. Tang, J. Wang, Q. Yi, *Front. Energy* **2024**, *18*, 42–53.
- [152] Q. Tang, Y. Zhang, N. Xu, X. Lei, K. Huang, *Energy Environ. Sci.* **2022**, *15*, 4659–4671.
- [153] S. Trocino, M. Lo Faro, S. C. Zignani, V. Antonucci, A. S. Aricò, *Appl. Energy* **2019**, *233–234*, 386–394.
- [154] S. Zhang, Y. Yang, L. Cheng, J. Sun, X. Wang, P. Nan, C. Xie, H. Yu, Y. Xia, B. Ge, J. Lin, L. Zhang, C. Guan, G. Xiao, C. Peng, G. Z. Chen, J.-Q. Wang, *Energy Storage Mater.* **2021**, *35*, 142–147.
- [155] H. Wang, B. Sun, C. Peng, *J. Electrochem. Soc.* **2024**, *171*, 070530.
- [156] S. Trocino, S. C. Zignani, M. Lo Faro, V. Antonucci, A. S. Aricò, *Energy Technol.* **2017**, *5*, 670–680.
- [157] T. Wang, T. Yang, D. Luo, M. Fowler, A. Yu, Z. Chen, *Small* **2024**, *20*, 2309306.
- [158] M. Jacob, K. Wissel, O. Clemens, *Mater. Futures* **2024**, *3*, 012101.
- [159] L. Schwich, M. Küpers, M. Finsterbusch, A. Schreiber, D. Fattakhova-Rohlfing, O. Guillon, B. Friedrich, *Metals* **2020**, *10*, 1523.
- [160] E. V. Timofeeva, C. U. Segre, G. S. Pour, M. Vazquez, B. L. Patawah, *Curr. Opin. Electrochem.* **2023**, *38*, 101246.
- [161] Z. W. Seh, J. Kibsgaard, C. F. Dickens, I. Chorkendorff, J. K. Nørskov, T. F. Jaramillo, *Science (1979)* **2017**, *355*, DOI 10.1126/science.aad4998.
- [162] M. Gao, C. Li, R. Wang, S. Xiao, Z. Guo, Y. Wang, *Next Mater.* **2024**, *2*, 100126.
- [163] S. R. Narayan, A. Manohar, S. Mukerjee, *Interface Mag.* **2015**, *24*, 65–69.
- [164] K. B. Ibrahim, M. Tsai, S. A. Chala, M. K. Berihun, A. W. Kahsay, T. A. Berhe, W. Su, B. Hwang, *J. Chin. Chem. Soc.* **2019**, *66*, 829–865.
- [165] J. Fan, J. Pan, H. Wang, S. Liu, Y. Zhan, X. Yan, *Adv. Funct. Mater.* **2024**, *2417580*.
- [166] P. N. Ross, H. Sokol, *J. Electrochem. Soc.* **1984**, *131*, 1742–1750.
- [167] P. Trogadas, T. F. Fuller, P. Strasser, *Carbon N Y* **2014**, *75*, 5–42.
- [168] L. Dai, *Acc. Chem. Res.* **2013**, *46*, 31–42.
- [169] Z. Zhao, M. Li, L. Zhang, L. Dai, Z. Xia, *Adv. Mater.* **2015**, *27*, 6834–6840.
- [170] K. Tang, H. Hu, Y. Xiong, L. Chen, J. Zhang, C. Yuan, M. Wu, *Angew. Chem. Int. Ed.* **2022**, *61*, e202202671.
- [171] S. Islam, S. M. A. Nayem, A. Anjum, S. Shaheen Shah, A. J. S. Ahammad, M. A. Aziz, *Chem. Rec.* **2024**, *24*, DOI 10.1002/tcr.202300017.
- [172] J. Pan, Y. Y. Xu, H. Yang, Z. Dong, H. Liu, B. Y. Xia, *Adv. Sci.* **2018**, *5*, 1700691.
- [173] C. Song, C. Huang, H. Xu, Z. Zhang, T. Shuai, Q. Zhan, G. Li, *Small* **2024**, *20*, 2402761.
- [174] Y.-F. Guo, L.-L. Zhao, N. Zhang, P.-F. Wang, Z.-L. Liu, J. Shu, T.-F. Yi, *Energy Storage Mater.* **2024**, *70*, 103556.
- [175] Y. Arafat, M. R. Azhar, Y. Zhong, H. R. Abid, M. O. Tadzé, Z. Shao, *Adv. Energy Mater.* **2021**, *11*, 2100514.
- [176] K. R. Yoon, K. Shin, J. Park, S.-H. Cho, C. Kim, J.-W. Jung, J. Y. Cheong, H. R. Byon, H. M. Lee, I.-D. Kim, *ACS Nano* **2018**, *12*, 128–139.
- [177] G. Sun, Q. Zhao, T. Wu, W. Lu, M. Bao, L. Sun, H. Xie, J. Liu, *ACS Appl. Mater. Interfaces* **2018**, *10*, 6327–6335.

Manuscript received: November 11, 2024

Revised manuscript received: January 31, 2025

Version of record online: March 17, 2025